

Original Article

An Intelligent Power Management and Power Quality Enhancement for Grid Integrated Renewable Sources and EV Fed UPQC

Alvala Mahesh Kumar¹, Sukhdeo Sao², E. Vidya Sagar³

^{1,3}Department of Electrical Engineering, UCE-Osmania University(A), Telangana, India.

²Department of Electrical Engineering, Vasavi College of Engineering, Telangana, India.

¹Corresponding Author : maheshkumarouphd@gmail.com

Received: 17 August 2023

Revised: 19 September 2023

Accepted: 15 October 2023

Published: 31 October 2023

Abstract - In recent years, integrating Renewable Energy Sources (RES) and Electric Vehicles (EVs) has significantly impacted distribution systems. The primary objective of this study is to address effectively the Power Quality (PQ) issues like sag, swell, and THD of a grid-connected system that combines Solar Photovoltaic (SPV) and Wind Energy Systems (WES), incorporating a Battery Energy Storage System (BESS) as well as Electric Vehicles (EVs) by using multi-functional Unified Power Quality Conditioner (UPQC) i.e (U-SWBEV) in addition to the power flow management between the RES, BESS, EV and grid. An Electric Vehicle Accumulator (EVAC) has been developed to address this. The suggested EVA is intended to integrate SPV, WES, BESS, and EVs. This integration aims to achieve several advantages, including an uninterrupted supply of power, meeting the electricity demand effectively and effective use of generated power. The regulation of power transfer from the generation to a consumer load, EVs, as well as between many sources and vice versa, is facilitated by using Artificial Neuro-Fuzzy Interface System (ANFIS) regulation, takes together the abilities of Fuzzy Logic (FL) and Artificial Neural Network (ANN). In addition, ANFIS is adopted to extract Maximum Power Point Tracking (MPPT) from the SPV system. During load change, there is a reduction in PQ at the load side. The most significant finding from the analysis and results is that the power output of the ANFIS-based MPPT is superior to the fuzzy logic-based MPPT. Thus, ANFIS and UPQC assist in achieving the efficient and proper use of power by effectively addressing PQ issues.

Keywords - Power Quality, ANFIS, Electric Vehicle Accumulator, ANN, Power management.

1. Introduction

In recent years, integrating renewable energy systems like solar and wind into the distribution network has been encouraged to reduce the stress on converters and ratings. The solar-integrated UPQC was developed to address PQ issues efficiently. The referenced study provides a comprehensive overview of the challenges linked to Renewable Energy Sources (RESs) and the strategies to address these issues [1-3]. The variability inherent in PV systems introduces harmonic distortion into the grid, leading to load voltage and current distortion. Consequently, FACTS devices were employed to mitigate THD and address voltage stability concerns. FACTS devices like UPFC, SVC, and UPQC are frequently applied to enhance PQ. Integrating FACTS devices effectively resolves voltage stability problems and enhances grid PQ [4-6].

1.1. Literature Survey

The utilization of the UPQC for a grid-tied SPV power system was examined to improve PQ [7]. A detailed

discussion was conducted on the functions of Electric Vehicles (EVs), charging strategies, and their associated advantages [8-10]. In the real-time FACTS, the UPQC outperforms the multi-functions of DSTATCOM and DVR. The UPQC effectively satisfies most of the required attributes, voltage profile enhancement, THD suppression, power factor improvement, and overall enhancement of the system's PQ [11].

The BESS-associated EV system utilizing FLC was introduced to deliver superior PQ, enhancing the overall reliability of the grid-tied SPV-WES-BESS-EVs system when contrasted to the primary grid system [12]. The solar system associated with UPQC was designed to handle PQ problems with the optimal selection of PI controller parameters and filter parameters using soccer league optimization [13]. The novel ANN controller-based reference signal generation was introduced to the UPQC with fuzzy controller-based ANFIS to maintain the DC link stable and handle PQ issues effectively [14]. The wind and battery associated UPQC with



the fuzzy controller was designed to solve PQ voltage and current problems. Additionally, to exhibit the system's viability, different test cases were selected for various load combinations [15]. The solar battery-based UPQC was developed with meta-heuristic algorithm-trained ANN was suggested to address PQ troubles [16].

The solar battery-based UPQC was created with soccer league algorithm-trained ANN meant to address PQ troubles [17]. The ANFIS-based hybrid controller was adopted for the wind battery system connected to a shunt active power filter to reduce THD effectively [18]. The hybrid control system incorporates both the FLC and ANN. The neuro-fuzzy hybrid controller was specifically designed to standardize the DC-link voltage. The primary goals of the recommended project were to reduce the presence of distortions in the current signal and improve the PF. Additionally, the work aims to quickly respond to changes in the demand load control voltage, eliminate voltage fluctuations in the power source, enhance performance during significant disruptions, and provide appropriate correction for imbalance systems [19-21].

1.2. Research Gap and Key Contributions

From the literature, it is evident that most of the literature papers mainly focused on UPQC with renewable sources like SPV WSS, in association with the BESS with various control techniques. However, they neglected EV integration into the system, but it is evident that during the grid's highest electricity demand periods, surplus power demand is addressed using BESS and EVs.

The contributions of this work are highlighted below in points:

- Design of Electric vehicle accumulator for appropriate power flow management among EVs, BESS and RES using ANFIS-based hybrid technique.
- Implementation of ANFIS technique for MPPT in PV system for extracting maximum output.
- Reduction of the Source current and load voltage THD and elimination of grid voltage side issues like (disturbance, swell, sag, etc) using U-SWBEEV.
- Integrating RES, EV and BESS for UPQC to reduce the stress and burden on VSC supports to meet the load demand and maintain constant DC link's voltage at irradiation and load variations.

In addition, the suggested ANFIS scheme for EVA and MPPT is examined on two test cases for different loading and irradiation conditions to show its superior performance concerning the minimization of current waveform THD and voltage waveform fluctuations.

1.3. Paper Alignment

The paper is structured as follows: Section 2 delves into the modeling of U-SWBEEV. Section 3 comprehensively

covers the techniques employed in research with the ANFIS technique. Section 4 provides Shunt and Series Controllers of UPQC. Section 5 defines the results with discussions. Finally, in Section 6, we conclude the work and outline potential future avenues for research in this field.

2. Design of Proposed U-SWBEEV

Figure 1 depicts the schematic structure of the suggested system. The integration of the grid with the SPV, WES, BESS, and EVs is achieved by employing a phase inverter. The UPQC is a device that integrates shunt and series VSCs. The job of the series filter is to mitigate voltage-related troubles on the grid side.

This is achieved by providing the necessary V_{sc} through the injecting transformer via L_{sc} . Similarly, the shunt filter is electrically connected to the grid via the L_{sh} . The SHAPF aims to mitigate the existing harmonics in the waveform by introducing appropriate compensatory current and ensuring a consistent DC link voltage.

However, the main advantage of external renewable source support is that it reduces the required ratings and stress of the converters. The SPV, WES, BESS, and EV parameters selected are listed in Table 1. Equation (1) calculates the dispersal of power, and an explanation is given in Table 2.

$$P_{PV} + P_{BESS} + P_w + P_{EV} = P_L \tag{1}$$

Where, P_{PV} denotes SPV output power,
 P_w denotes WES output power,
 P_{BESS} denotes energy storage battery output power,
 P_{EV} denotes the output power of the EV,
 P_L denotes the output power of the Load.

2.1. SPV Structure

The SPV transfers sun irradiation to electricity, depending on the number of PV modules connected in series and parallel. PV models are arranged in series to create a string, and multiple strings are connected in parallel to produce the necessary voltage and current. Within each module, a single diode equivalent circuit represents each PV cell, as shown in Figure 2.

It comprises a photocurrent source (i_p) with a forward diode (i_d) conducting current, along with series and parallel resistances ($R_{s,PV}$ and $R_{sh,PV}$) that carry currents (i_{PV} , $i_{sh,PV}$). The PV cell detects solar irradiation and transforms it into current. Using KCL, the PV cell's current at output (i_{PV}) is determined as per Equation (2).

$$i_{PV} = i_{ph} - i_d - i_{sh,PV} \tag{2}$$

$$i_{PV} = i_p - i_{sat} \left[\exp\left(\frac{Q(V_{PV} + (i_{PV}R_{s,PV}))}{\eta k T_C}\right) - 1 \right] - \frac{V_{PV} + (i_{PV}R_{s,PV})}{(R_{sh,PV})} \tag{3}$$

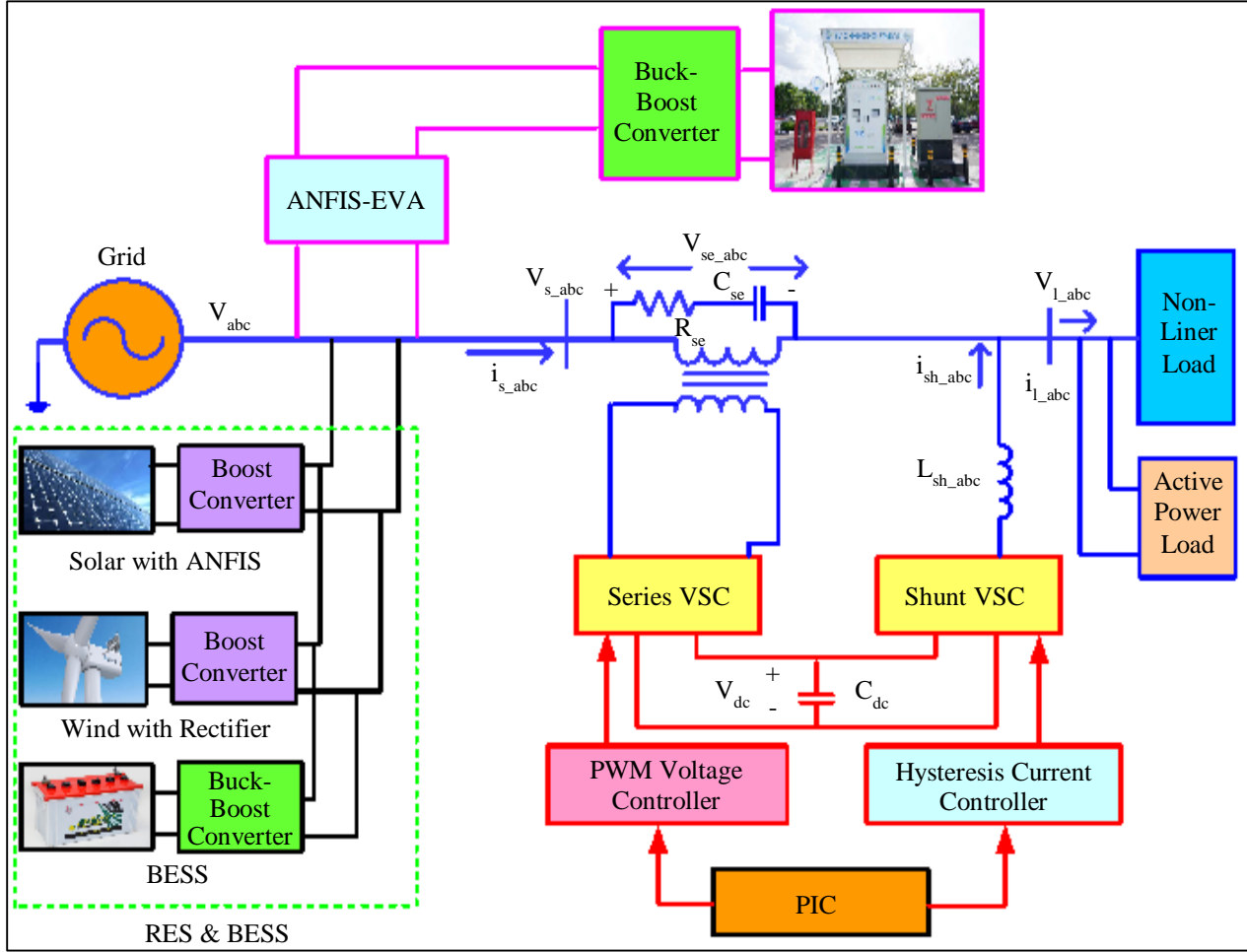


Fig. 1 Proposed U-SWBEV configuration

Table 1. PV, Wind, BESS, and EV selected ratings

Device	Configuration	Values
PV single panel (Sun power SPR-215-WHT-U)	PV cells connected in parallel, series	45, 10
	Rated power	228.735W
	Short circuit current	8.18A
	Open circuit voltage	37.1V
	Under max power, the voltage & current	29.9V /7.65A
Li-ion battery	Fully charge voltage	326.6V
	Rated capacity of battery	400Ah
	Cut off voltage	225 V
	Normal voltage	300V
	SOC	95%
Wind turbine	Nominal turbine mechanical power	30 KW
	Maximum pitch angle	45deg.
	Base wind speed	15 m/sec
	Maximum rate of change of pitch angle	25deg./second
	Pitch angle K_i	5
	Pitch angle K_p	25

In this context, i_{sat} represents the reverse saturation current, Q represents the charge of an electron, the diode's ideal factor, k denotes Boltzmann's constant, and T_C represents the cell's temperature. Additionally, $V_{PV,c}$ and $i_{PV,c}$ refer to the voltage as well as current output of the cell. In the literature, most of the conventional systems focus mainly on the P&O method is adopted. However, to enhance PV output, the ANFIS-based MPPT is adopted in this work. The solar irradiation and temperature were inputs for the proposed ANFIS technique, and the duty cycle is considered output (discussed in detail section 3.1). The output power obtained from the solar system (P_{PV}) is calculated by Equation (4). The control system of PV and characteristics are illustrated in Figures 3 and 4, respectively.

$$P_{PV} = V_{PV} \cdot I_{PV} \tag{4}$$

2.2. BESS

The BSS gives support for power management to satisfy load. To obtain the required current/ voltage, batteries are

made up of cells arranged in series or parallel. Because lead-acid batteries have low maintenance costs, they are chosen from the Simulink library for this work. Equation (5) represents the Li-ion battery's charging and discharging model.

$$V_b = E_{fl,2}(i_t, i_b, i_b) - iR \tag{5}$$

Where, $E_{fl,2}(i_t, i_b, i_b)$ there is no load voltage, 'R' is the value of internal resistance, i_b battery current.

The State of Charge in Battery (SOCB) is expressed in Equation (6).

$$SOCB = 95(1 + \int i_{BSS} dtQ) \tag{6}$$

The SPG will decide whether the battery is charged or discharged while satisfying the constraints given by Equation (7). The discharge of the battery is shown in Figure 5.

$$SOCB_{min} \leq SOCB \leq SOCB_{max} \tag{7}$$

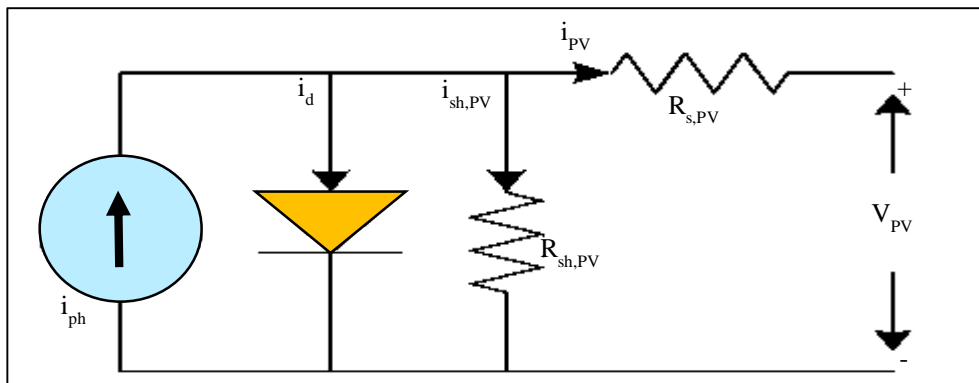


Fig. 2 PV cell single diode model

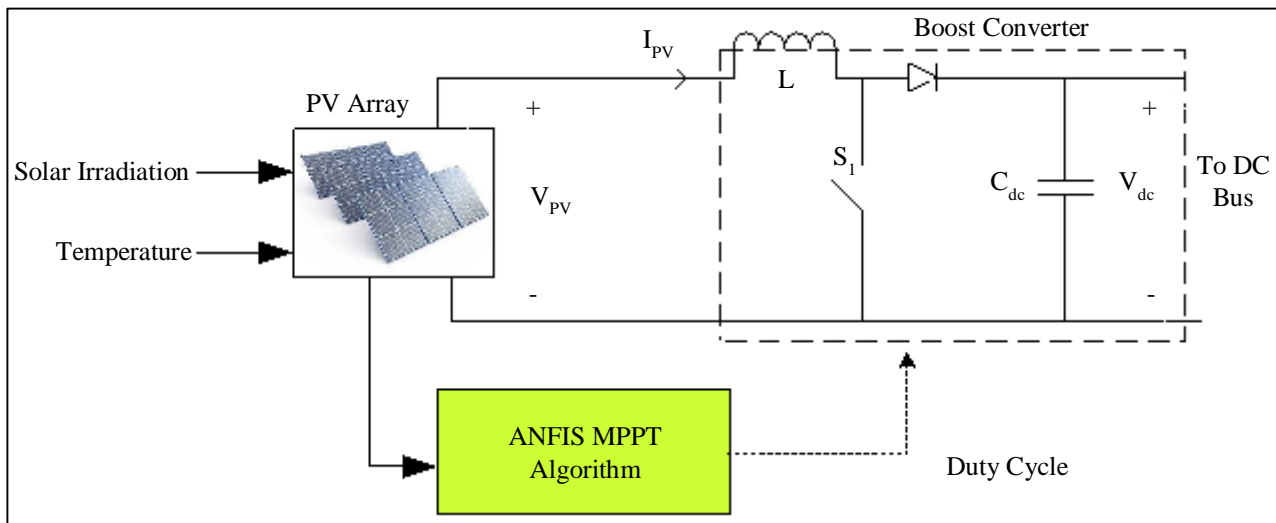


Fig. 3 Solar control system with B-C

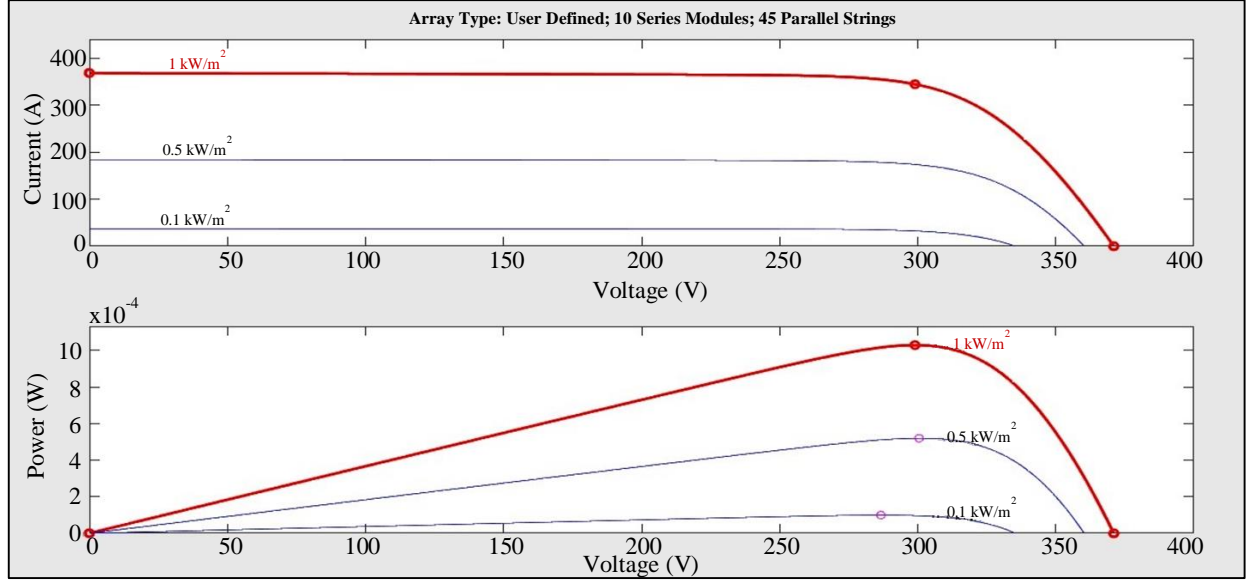


Fig. 4 Variable irradiation constant temperature characteristic

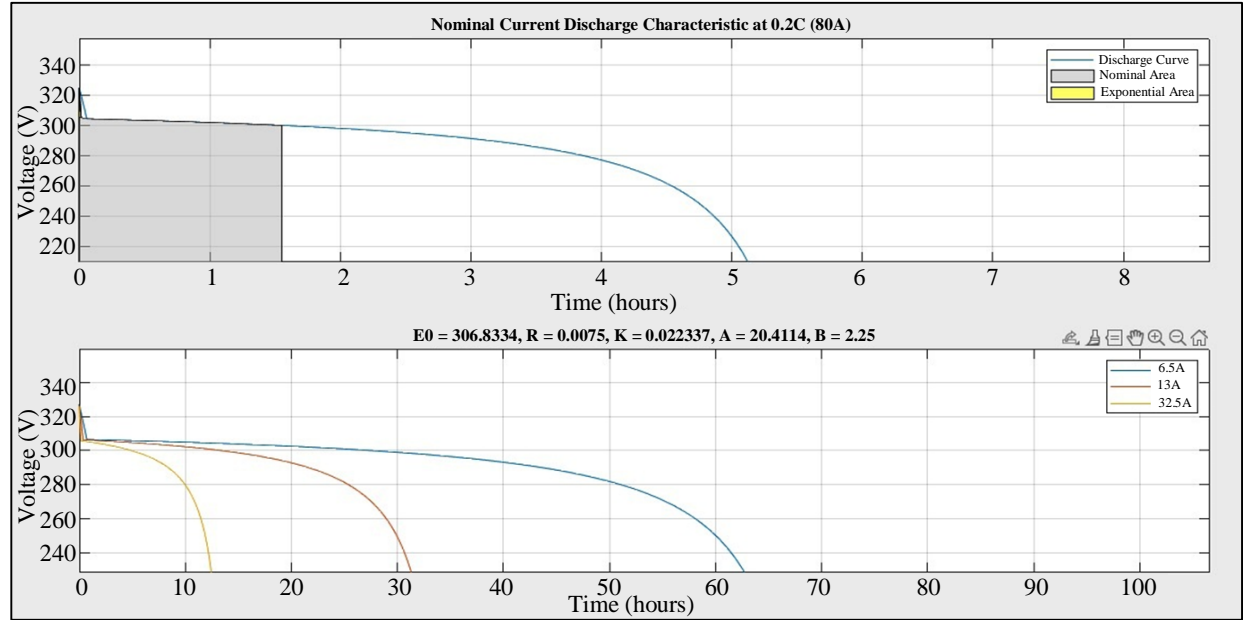


Fig. 5 Battery discharge characteristics

2.3. Wind System

The AC voltage produced by the wind is converted into DC voltage through rectification, and this DC voltage is subsequently increased using a boost converter. A permanent magnet synchronous machine is considered in this present work due to its efficiency, easy handling, lower cost, and reliability. Equations give the power generated by WES (8) - (12).

$$R_{st} = \omega R_b / V_w \quad (8)$$

$$P_{mop} = 0.5 \rho \pi R_b^2 C_{pc} V_w^3 \quad (9)$$

$$P_{mop} = \omega T_{mop} \quad (10)$$

$$C_p = (0.44 - 0.0167\theta_p) \sin \frac{3.14(N_r - 2)}{13 - 0.3\theta_p} \quad (11)$$

$$-0.0018(N_r - 2) = \theta_p \quad (12)$$

Here, ω denotes rotor velocity in rad/sec, V_w is the wind speed, R_b is the blade's radius, R_{st} tip speed ratio, and ρ indicates air density. The terms torque output (T_{mop}), mechanical power output (P_{mop}), and coefficient of power (C_p) are used to express these concepts. In Equation 11, the speed ratio is N_r , and the blade's pitch angle is θ_p .

3. ANFIS for Solar MPPT and to the Proposed EVA

It is essential to meet load demand for the reliable operation of power systems. ANFIS-based MPPT is adopted to extract maximum power from the SPV system, ANFIS technique-controlled EVA is developed for power management between RES and EVs, and UPQC is adopted to mitigate current and voltage-related PQ issues.

3.1. ANFIS Based MPPT

The ANFIS is an intelligent hybrid controller integrating ANNC and FLC features seamlessly. The inputs fed to the ANFIS are initially trained according to the Gaussian MSF to produce the best, as shown in Figure 6.

ANFIS mainly consists of five layers; the 1st layer (Fuzzification), the outputs of this layer are fuzzy Membership Function (MSF) given by Equation 13, shown in Figure 7.

$$\begin{aligned} \mu_{A_i}(x), i = 1,2. \\ \mu_{B_j}(y), j = 1,2. \end{aligned} \tag{13}$$

Where, μ_{A_i} , μ_{B_j} are the MSF outputs obtained from the 1st layer. The mathematical representation of Gaussian MSF is given by Equation 14. The inputs of MF are shown in Figure 6.

$$\mu(x) = e^{-\frac{(x-a)^2}{b}} \tag{14}$$

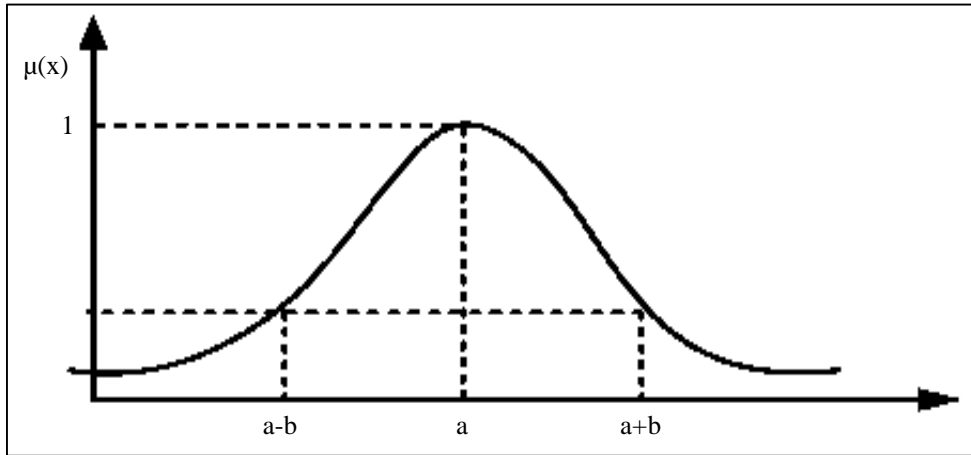
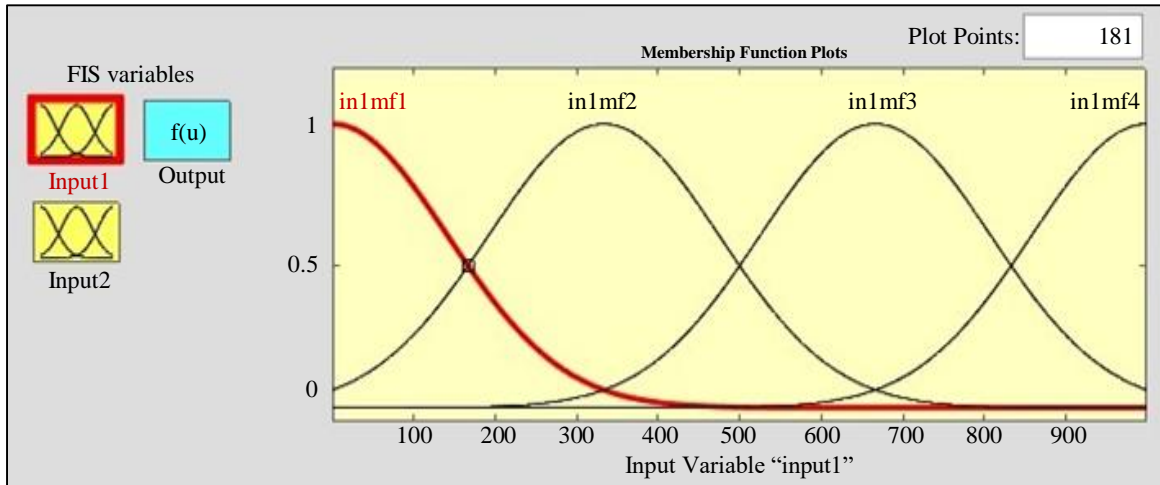
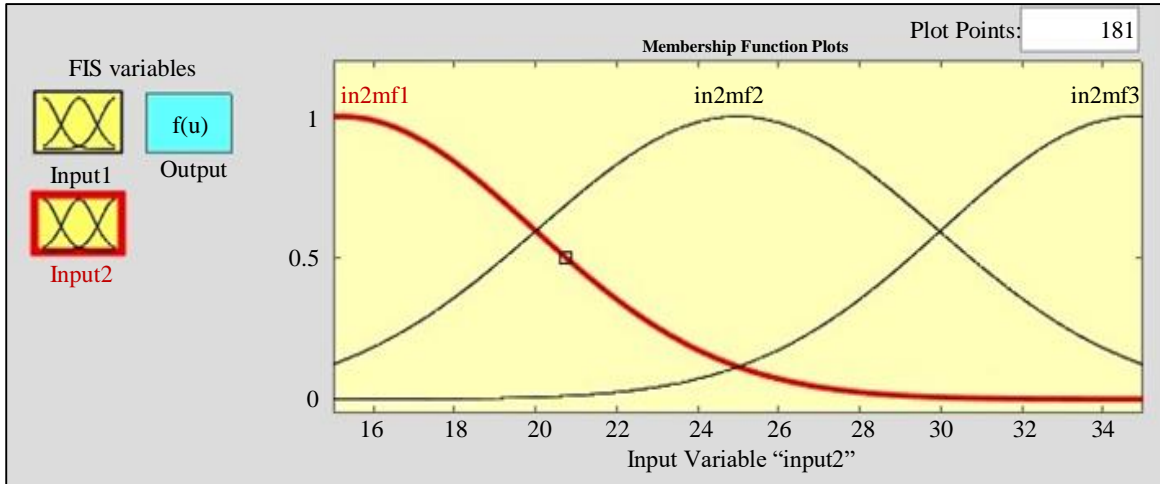


Fig. 6 Gaussian MSF



(a) MSF for input1



(b) MSF for input2
Fig. 7 MSF for inputs of MPPT

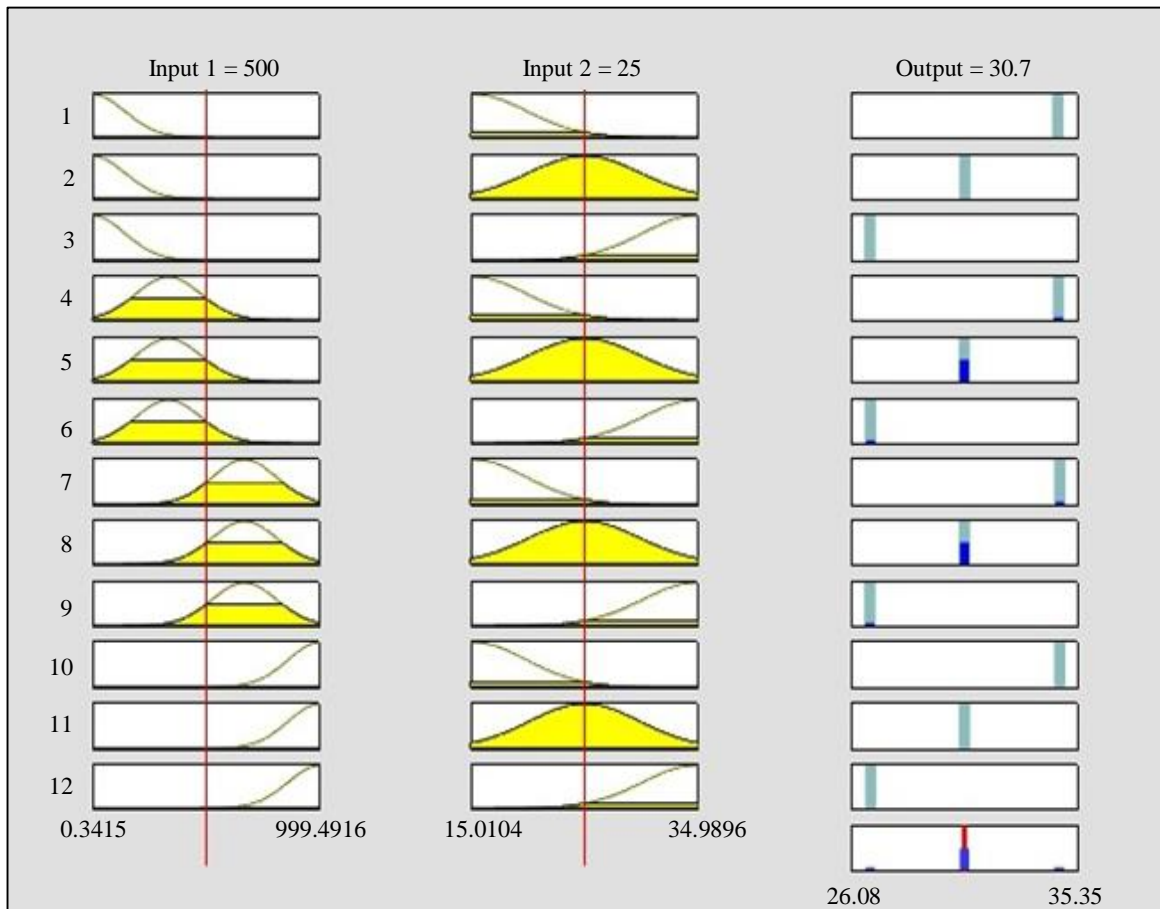


Fig. 8 MPPT rule base

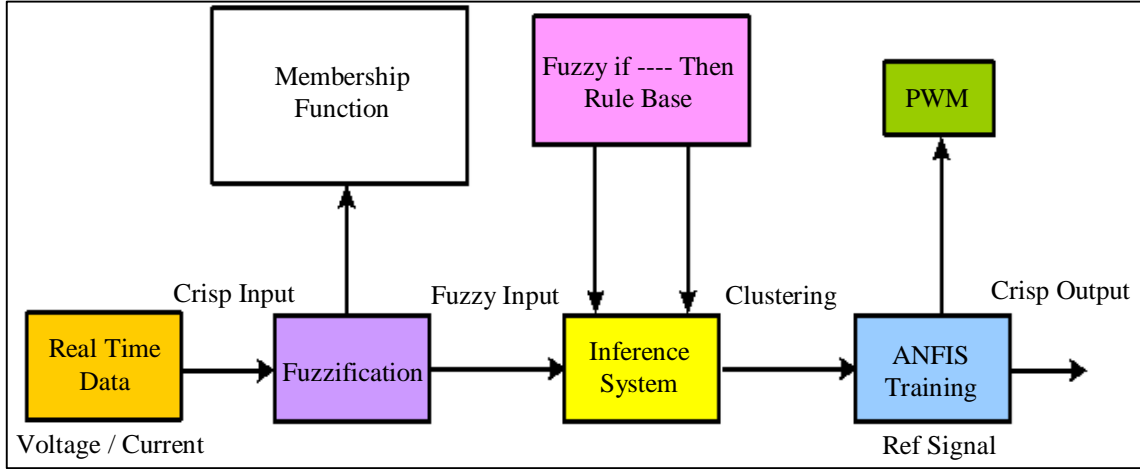


Fig. 9 Overview of ANFIS

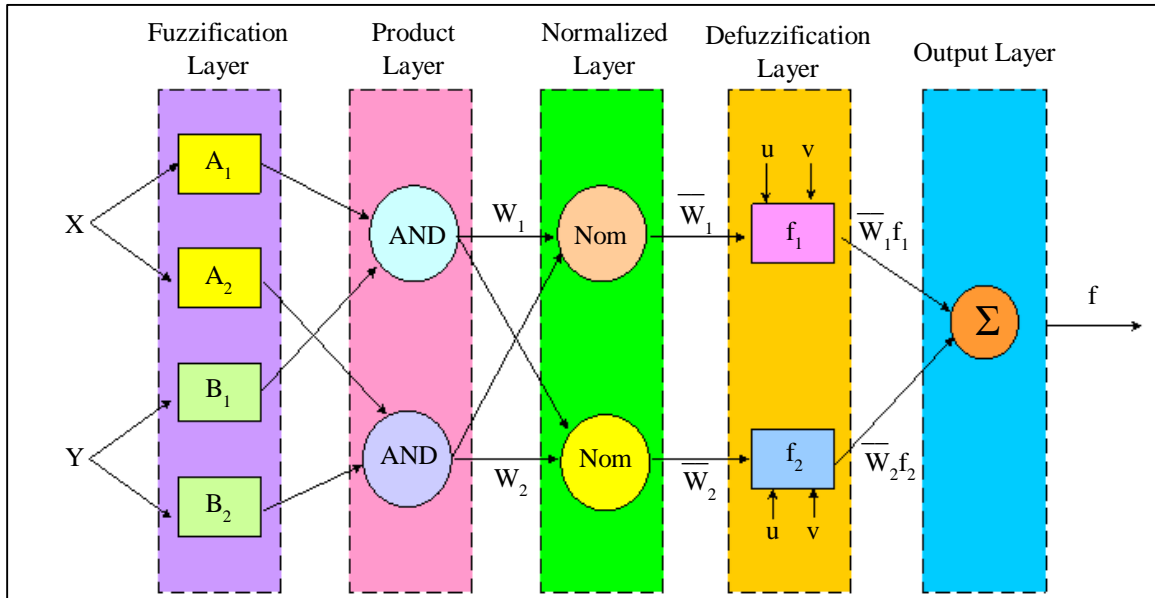


Fig. 10 Structure of ANFIS

However, in the 2nd layer (weighting of fuzzy rules), the AND operator is applied and calculates the firing strength w_i by adopting MSF computed in the 1st layer, whose output is calculated by Equation (15).

$$w_k = [\mu_{A_i}(x)] * \mu_{B_j}(y) \quad i, j = 1, 2. \quad (15)$$

The normalization of values occurs in the 3rd layer received from the previous layer. Each node reaches normalization by evaluating the ratio of the kth rule to the summation of all rule's the firing strength is given in Equation (16).

$$\bar{w}_k = \frac{w_k}{w_1 + w_2} \quad k = 1, 2. \quad (16)$$

The self-adaptive ability of the ANNC is carried out by applying the inference parameters (p_k, q_k, r_k) in the 4th layer (defuzzification) output given by Equation (17).

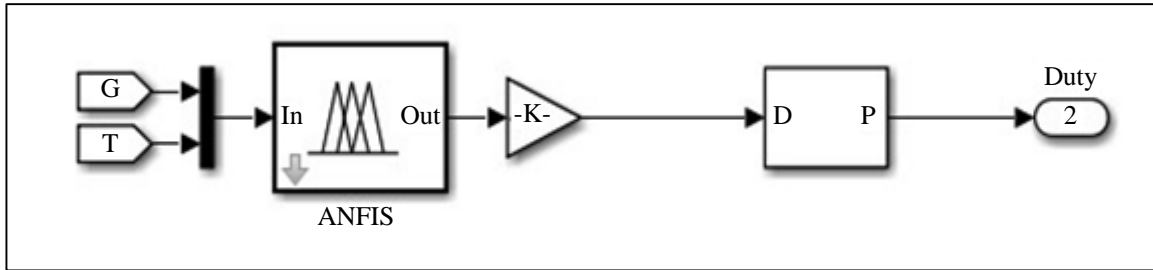
$$\bar{w}_i f_i = \bar{w}_i (p_k u + q_k v + r_k) \quad (17)$$

Lastly, at the 5th layer, inputs are added up to produce the desired total ANFIS output by Equation (18). Figures 9 and 10 show the overview and block diagram of the proposed ANFIS.

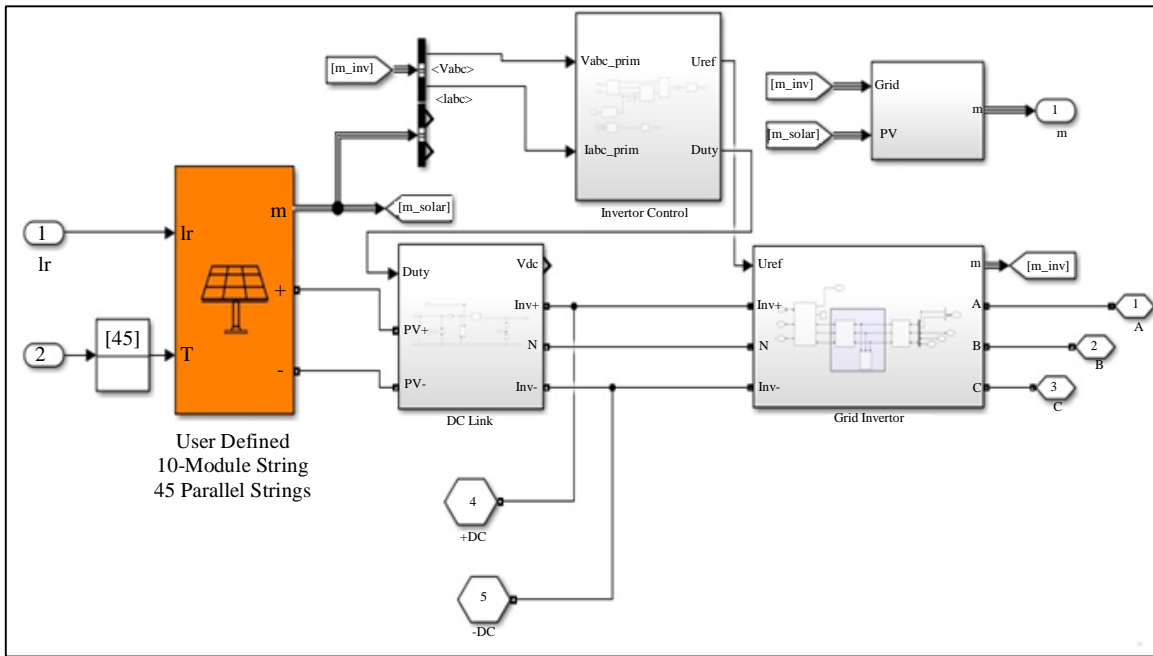
$$f = \sum_i \bar{w}_i f_i \quad (18)$$

The ANFIS is trained to reduce the root mean square error between the obtained and required output with the aim of extracting maximum output from the SPV system.

Here, the solar irradiation and temperature are inputs to the ANFIS and duty cycle as output to control the boost converter. The Matlab model of ANFIS-controlled MPPT with SPV is given in Figure 11.



(a) ANFIS controlled MPPT



(b) Solar PV simulation model

Fig. 11 Matlab/Simulink model ANFIS controlled MPP

3.2. ANFIS Controlled EVA for Power Management

With the aid of RES’s power generation forecasting, functions by overseeing the power flow between EVs and the grid, facilitating power transfer from EVs to the grid or from the grid to EVs. This study details how to improve power management and PQ in the grid system by integrating EVs and UPQC.

This indicates that the primary goal of implementing EVA is to control EV usage as transportable, temporary BESS. As a result, when using the stored energy as ESS is unnecessary, it can also be used for transportation. In this work, the suggested technique is controlled by the ANFIS hybrid technique.

The EVA power management system is designed using a hybrid controller, sometimes called an ANFIS controller, for performance analysis, which combines the best features of both fuzzy and artificial neural networks. Here, the flow chart

depicted in Figure 12 explains how the proposed ANFIS-based EVA operates. Information is exchanged between the EVA controller and the grid, RESs, ESS, and charging stations (ST1, ST2, ST3, ST4). EV charging decisions are made with the assistance of EVA.

If the EVs are not being driven, they stop at charging stations. During periods of high Load, these EVs might be utilized as ESS. Because these are employed as ESS, for some time longer than the grid’s peak load hour is lowered. The availability of EVs and their State of Charge (SOC) determine how much power EVs can offer to the grid.

The usage of ANFIS allows for the regulation of the flow of power to load from various available RES as well as from the BESS and EV systems. The MSF is illustrated in Figure 13. The power management with the proposed technique is highlighted in detail in Figure 14. The surface and rule base are given in Figures 15 and 16, respectively.

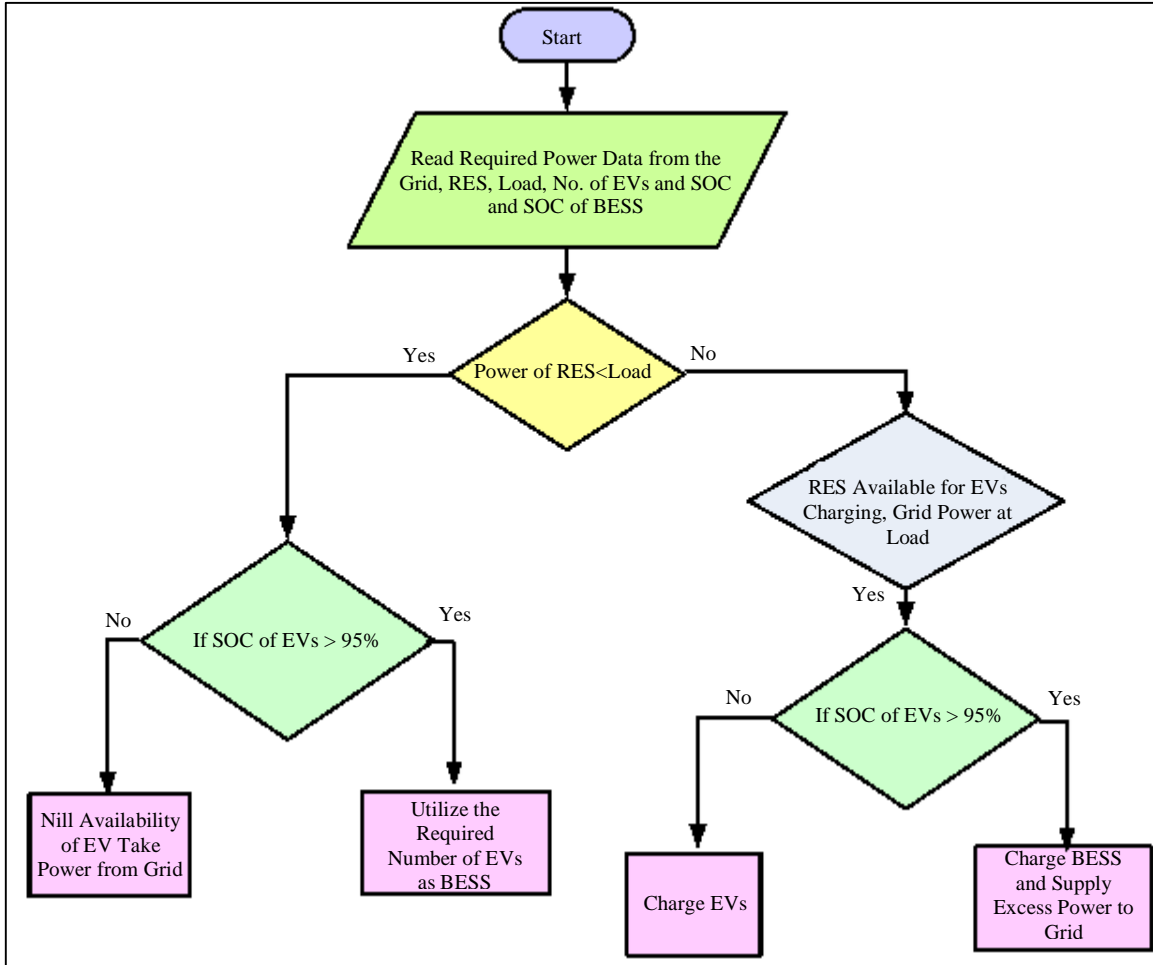
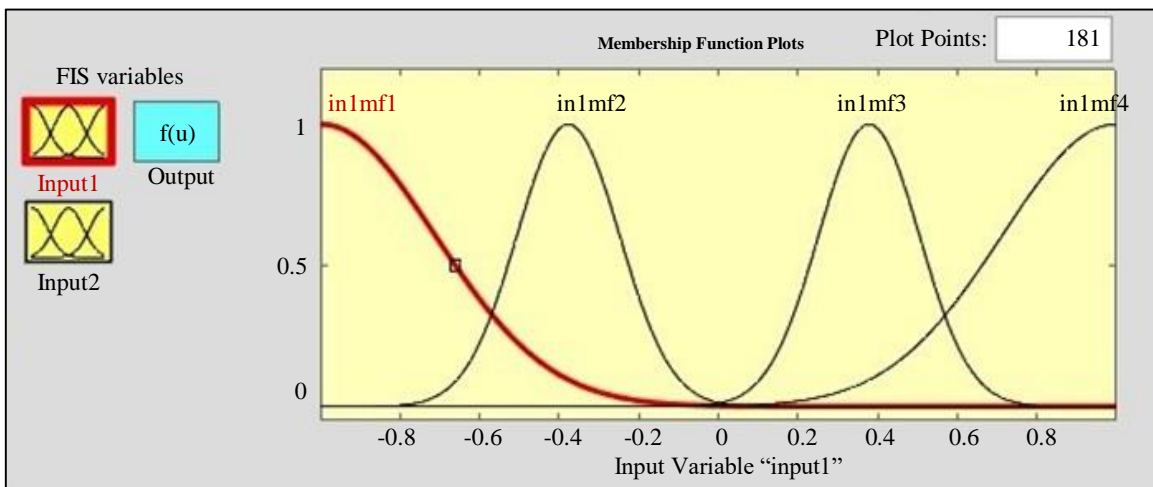
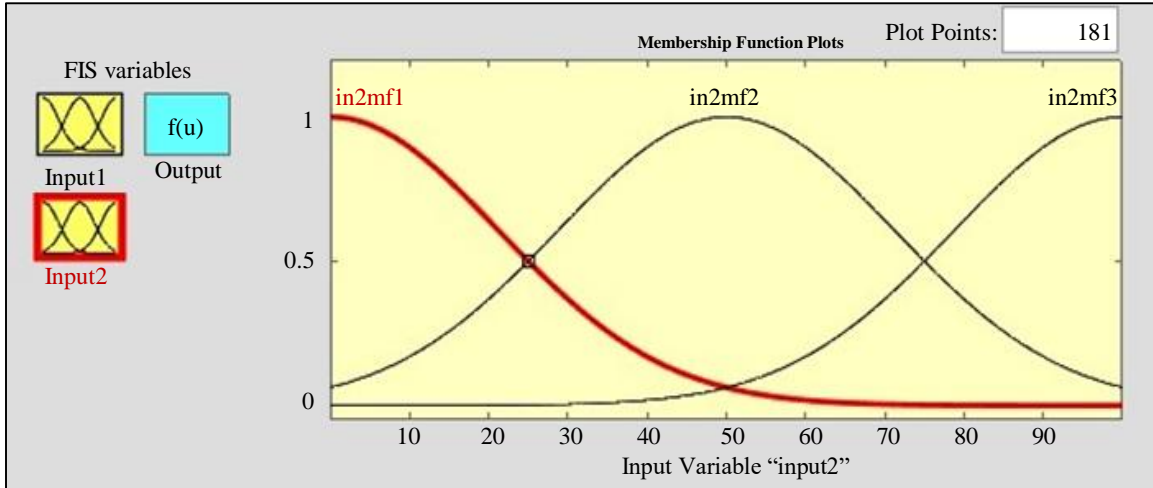


Fig. 12 Flow chart



(a) MSF for input1



(b) MSF for input2
 Fig. 13 MSF for inputs of EVA

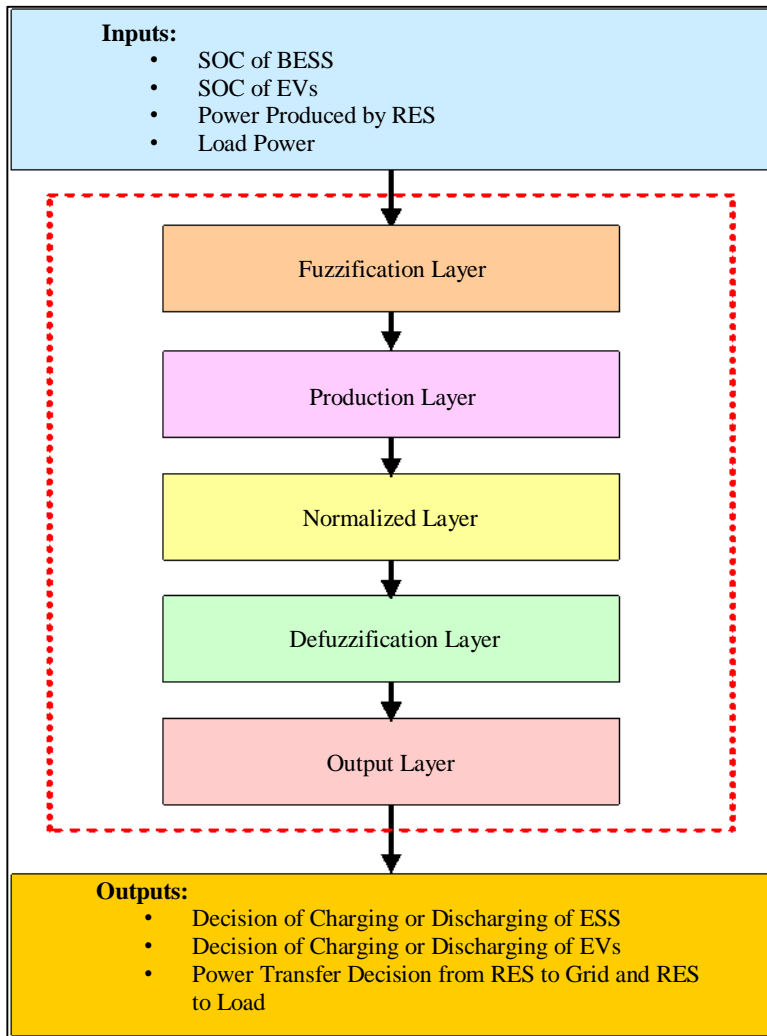


Fig. 14 ANFIS-controlled EVA for power management

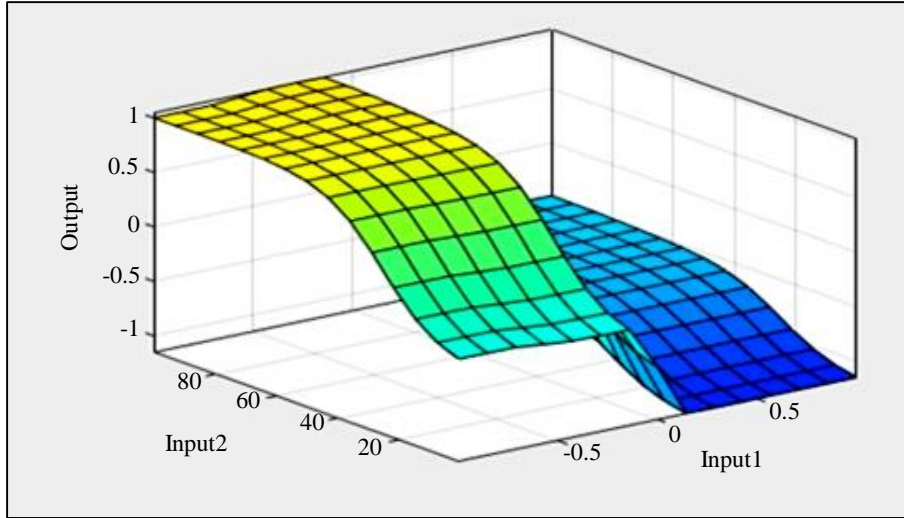


Fig. 15 EVA ANFIS surface

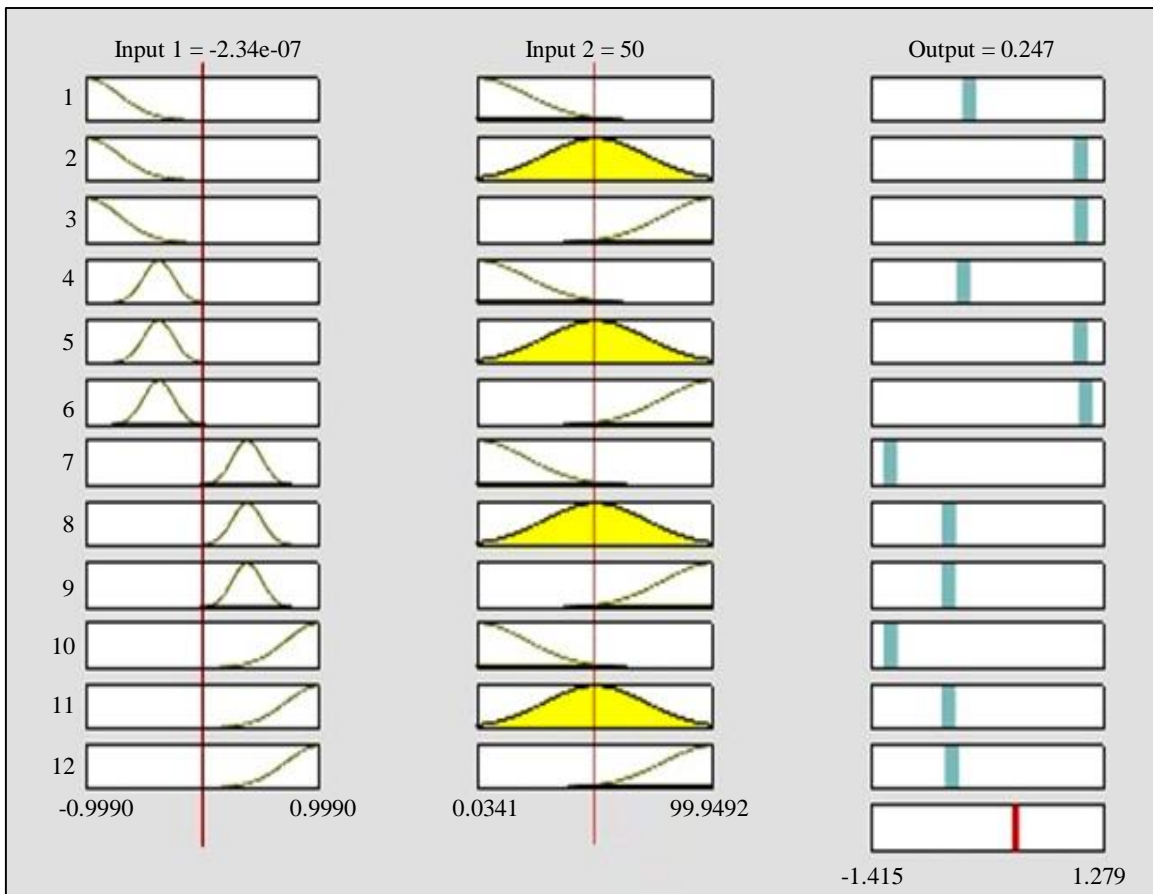


Fig. 16 EVA rule base

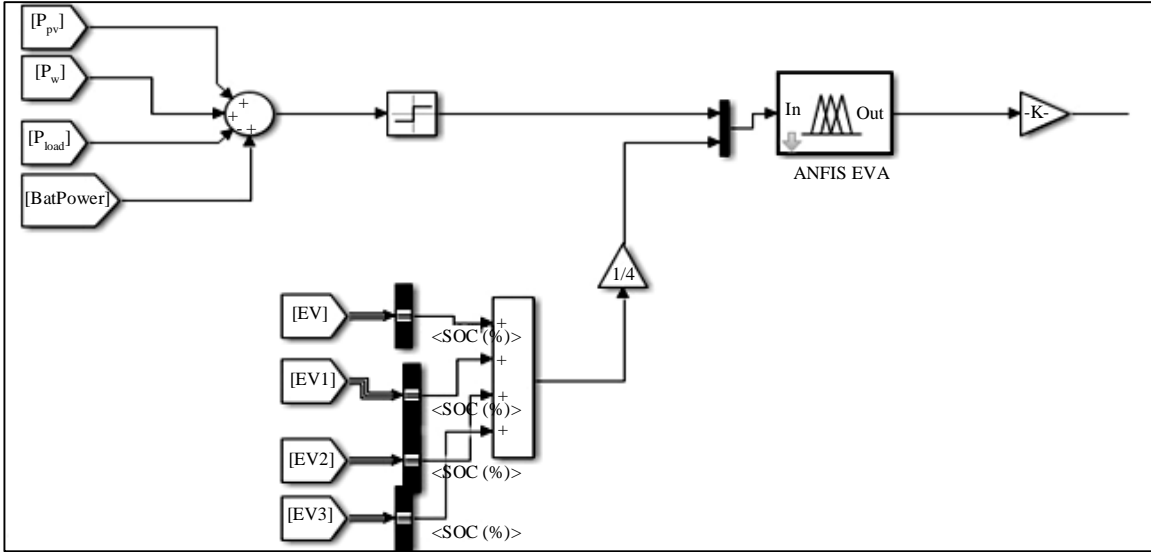


Fig. 17 Matlab/simulink of proposed EVA power management

4. Shunt and Series Controllers of UPQC

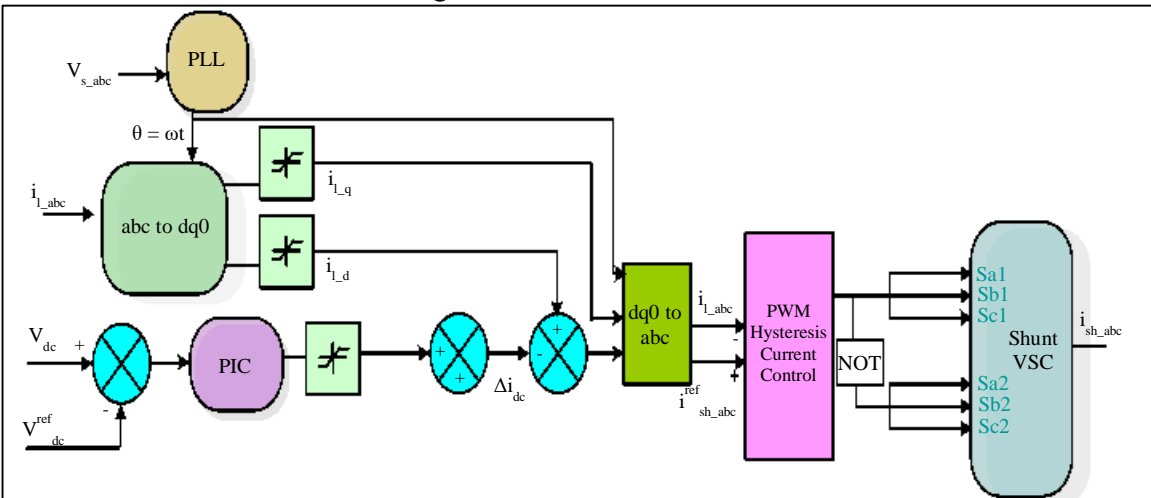


Fig. 18 Shunt converter control system

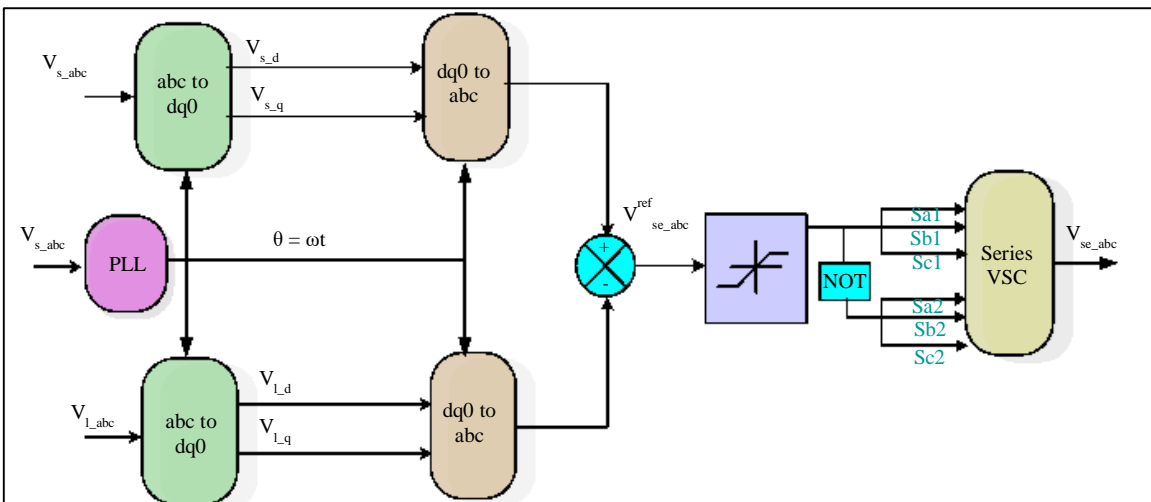


Fig. 19 Series converter control system

To reduce current harmonics and control DC-link voltage, the shunt SVC uses,

- (i) The dq0-abc and vice-versa shifting,
- (ii) Standard PIC.

The PLL uses the supply voltage’s phase and frequency information to convert the current at Load into the dq0. The PIC monitors the DC bus voltage against a predetermined reference value to maintain voltage regulation, and they translate any errors into the appropriate current adjustment. The qth part of the load current is added to PIC.

The Simulation of the suggested EVA is illustrated in Figure 17. To provide gate signals, the Hysteresis controller is adopted, as shown in Figure 18. Following the transformation from the abc to dq0 and subsequent conversion back to the abc, the voltage at loads is compared to a selected voltage. This comparison generates the necessary firing pulse generation adopting pulse width modulation, as depicted in Figure 19.

5. Results with Discussion

The developed U-SWBEV with ANFIS is designed in Simulink/Matlab 2022b. The selected system, UPQC-chosen parameters, and loads chosen are exhibited in Table 2. However, three case studies with various permutations of voltage issues like sag, disturbance, swell, loads with inconsistent irradiation and fixed temperature of 250c were selected to reveal the working of developed EVA on U-SWBEV. In this work, intelligent power management effectively addresses PQ issues, which is considered objective, obtained by creating ANFIS-based EVA for power management and UPQC for PQ. The THD is evaluated by Equation (19).

$$THD = \frac{\sqrt{I_2^2 + I_3^2 + \dots + I_n^2}}{I_1} \tag{19}$$

Where,
 I_n = individual harmonic current distortion values in amps,
 I_1 = individual harmonic current distortion values in amps,
 I_2 = 2nd harmonic current distortion values in amps.

Table 2. Grid system and UPQC parameters

Source Grid	V_s : 415V ; f : 50Hz
DC Link Capacitor & Coupling Inductors	V_{dc} : 470v ; C_{dc} : 100 μ F; R_{se} : 1ohm; C_{se} = 100 μ F, L_{sh} =10mH
Loads	Rectifier Bridge Load R = 60; L = 0.15e-3. Active Power Load: P_{L1} =2kW Active Power Load: P_{L2} =5 kW

Case 1 : Performance of proposed system under constant irradiation (1000W/m2) and temperature of 250c with loads 1& 2 with sag in source voltage.

In case 1, from Figure 20(a), it is observed that the proposed intelligent power management technique works effectively for the appropriate handling of EVs, depending on their SOC. Here, at 0.1sec, the grid takes power while PV and wind provide their outputs. However, during this condition, BESS charges and EVs discharge and supply the required power to the load and maintain constant power to the load. In addition, Figure 20(b) provides the irradiation, the maximum output power from the SPV system by ANFIS-based MPPT to maintain DC link voltage. Similarly, 20(c) exhibits that the series filter of UPQC works efficiently to remove sag by injecting the required voltage and maintaining the load voltage constant. Besides, the load current is highly polluted due to the nonlinear Load the shunt active power filter injects the current and maintains sinusoidal Source current as given in Figure 20(d).

Case 2 : Performance of proposed system under constant irradiation (1000W/m2) and temperature of 25⁰c with variation of Loads 1& 3 with harmonic condition in source voltage

In case 2, similar to case 1 from Figure 21(b), it is observed that the proposed intelligent power management technique is working effectively for the appropriate handling of EVs, depending on their SOC. At 0.23sec, the grid supplies power while RES provides its outputs. However, both BESS and EVs are charging here, and the grid with RES provides the required amount of energy to the load and maintains constant power to the load.

Figure 21(b) shows the irradiation, the maximum output power from SPV implementing ANFIS-based MPPT to maintain DC link voltage during the change in load condition. Meanwhile, 22(c) exhibits that the series filter of UPQC works efficiently to eliminate the harmonic distortion by injecting the required compensating voltage and maintaining the load voltage constant. Besides, the load current is highly polluted due to the nonlinear Load the shunt active power filter injects the current and maintains sinusoidal source current as given in Figure 21(d).

Case 3 : Performance of proposed system under variable irradiation and constant temperature of 25^o c with Loads 1& 2 with swell condition in source voltage.

In this case 3, variable solar irradiation is selected to observe the performance of the proposed method, as seen in Figure 22(a) the grid power is zero near 0.3 sec and RES provides supply while BESS is discharging mode and EVs in charging mode to satisfy load. Similarly, at 0.65 sec, PV power is almost negligible, but wind provides the power;

under this condition, BESS stands neutral, but EVs supply power to meet the load and the grid. Figure 22(b) shows the selected variable irradiation with power output and DC link balancing. However, similar to cases 1 and 2, the voltage swell condition was studied and compensated by UPQC effectively along with source current THD minimization, as shown in Figure 22(c) and (d).

Table 3 shows the THD of the proposed method in all case studies. It exhibits that the proposed method has a much lower THD within the IEEE standards. However, Figure 23 represents the FFT analysis of case 1 source current of the proposed system. Figure 24 illustrates the %THD comparison for the proposed system’s source current and Load voltage. It

exhibits that the proposed method has a much lower THD within the IEEE standards. Table 4 compares current THD with state of the art of literature.

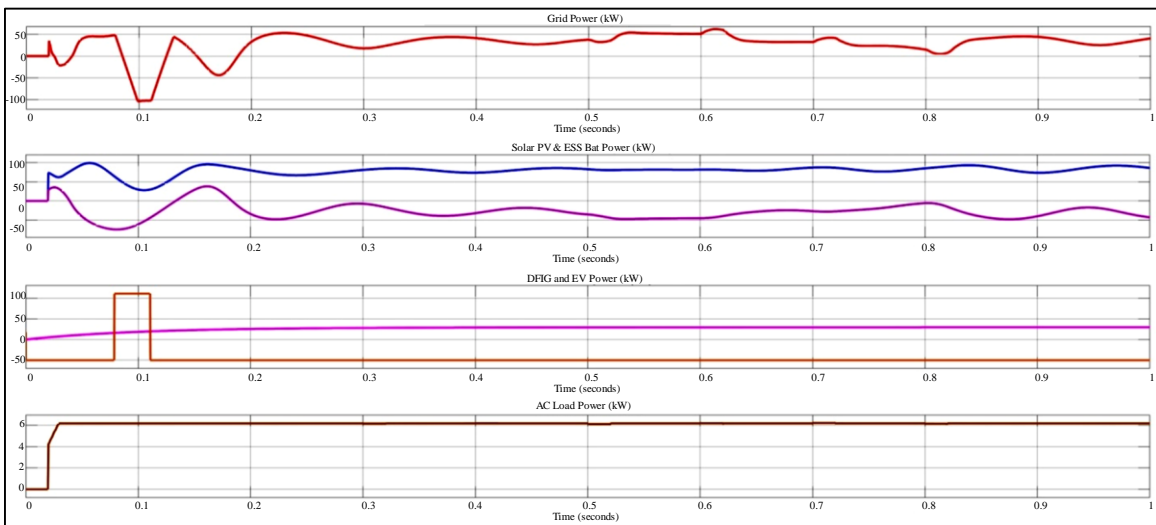
Table 3. % THD comparison

Case	THD	
	Source Current	Load Voltage
Case-1	0.84	0.30
Case-2	0.98	0.34
Case-3	0.69	0.33

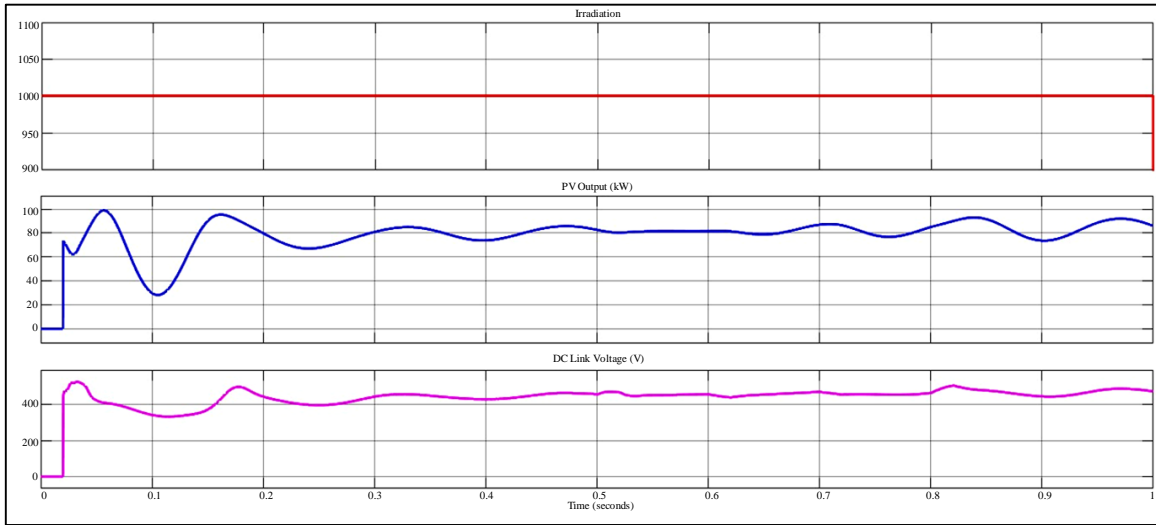
Table 4. % THD comparison with literature

Case	Controller / Ref []	THD	
		Source Current	Load Voltage
Case-1	DM	0.84	0.30
	[13]	2.06	--
	[14]	3.72	--
	[15]	1.60	--
	[16]	2.39	--
	[17]	2.40	--
	[18]	2.30	--
Case-2	DM	0.98	0.34
Case-3	DM	0.69	0.33

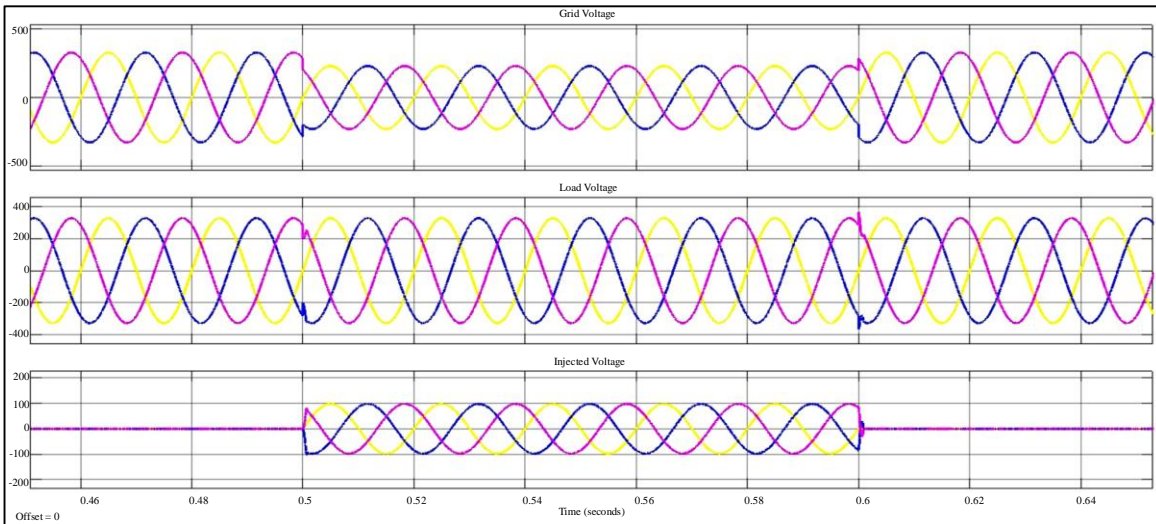
*DM is a developed method of ANFIS for EVA for UPQC



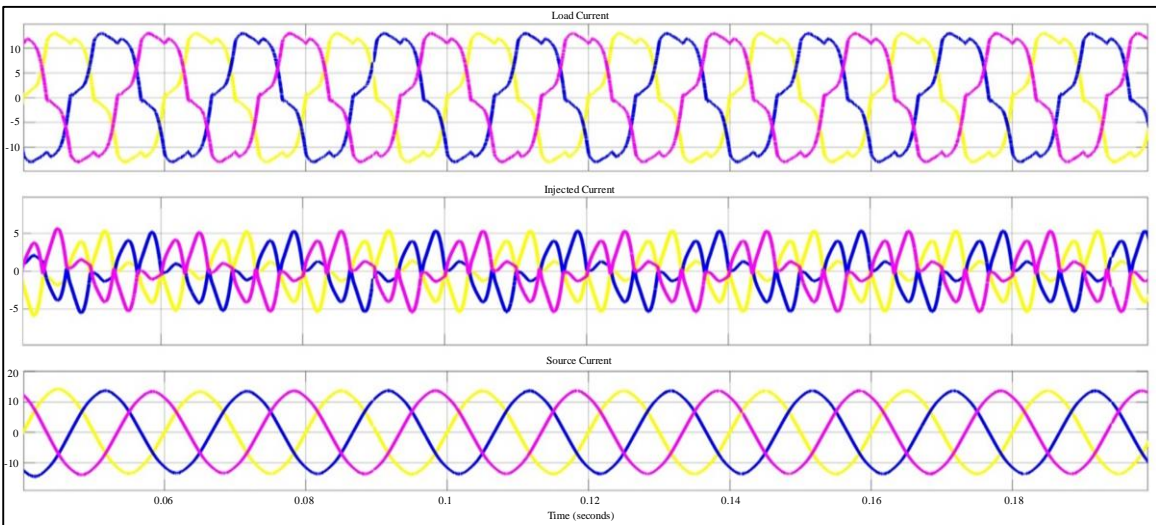
(a) Grid power, P_{PV}, P_{BESS}, P_w, P_{EV}, P_L



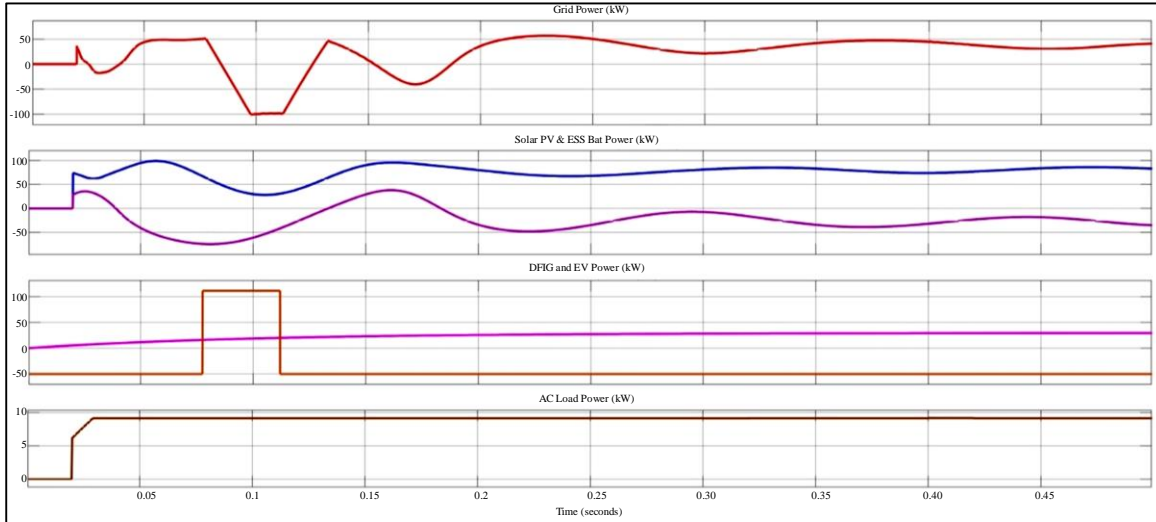
(b) G , P_{pv} , UPQC DC link voltage



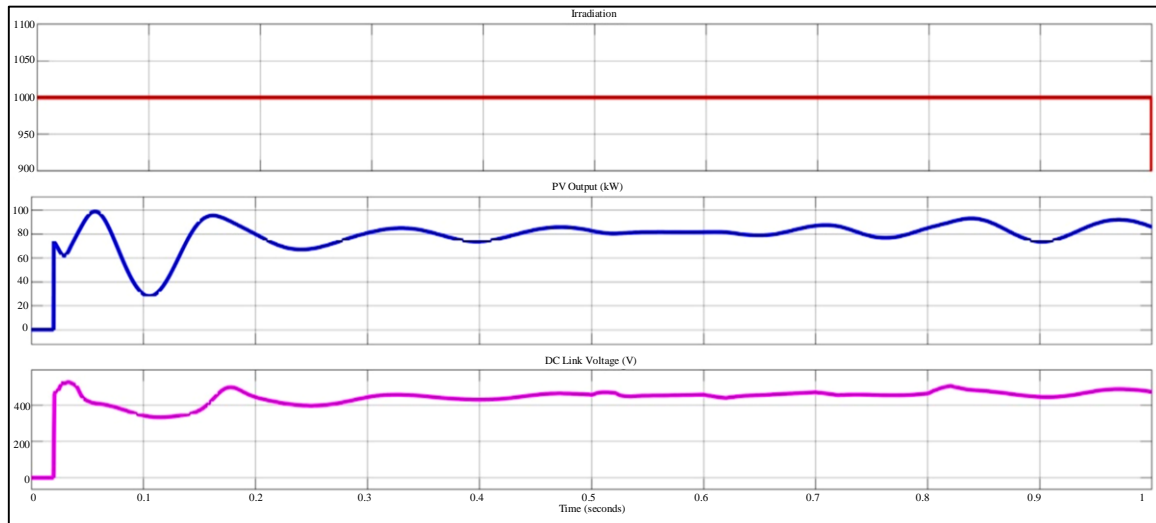
(c) Grid voltage, load voltage, series filter compensated voltage



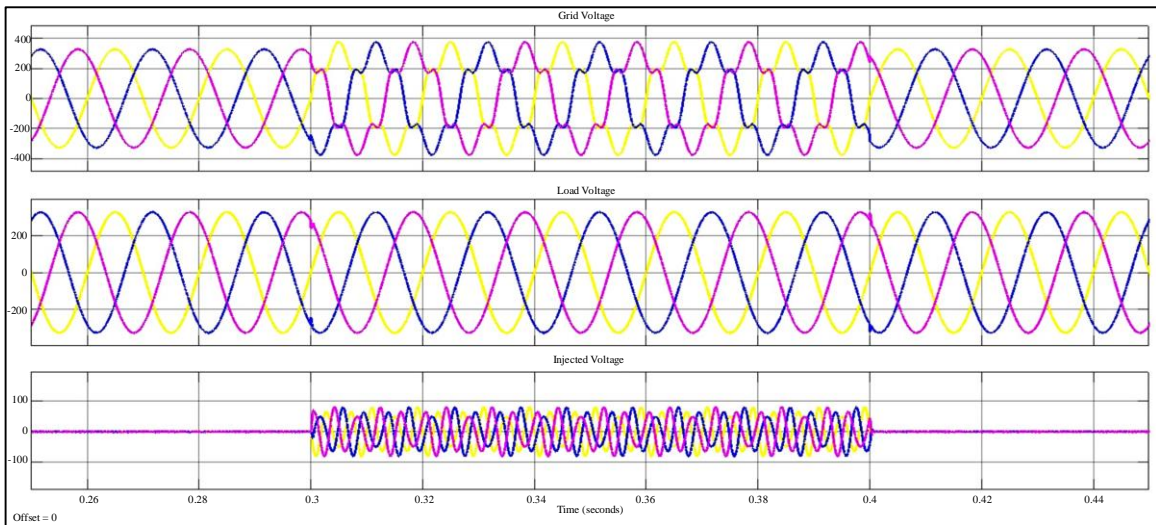
(d) Current at load, compensated current, source current
 Fig. 20 Waveforms of the developed method for case1



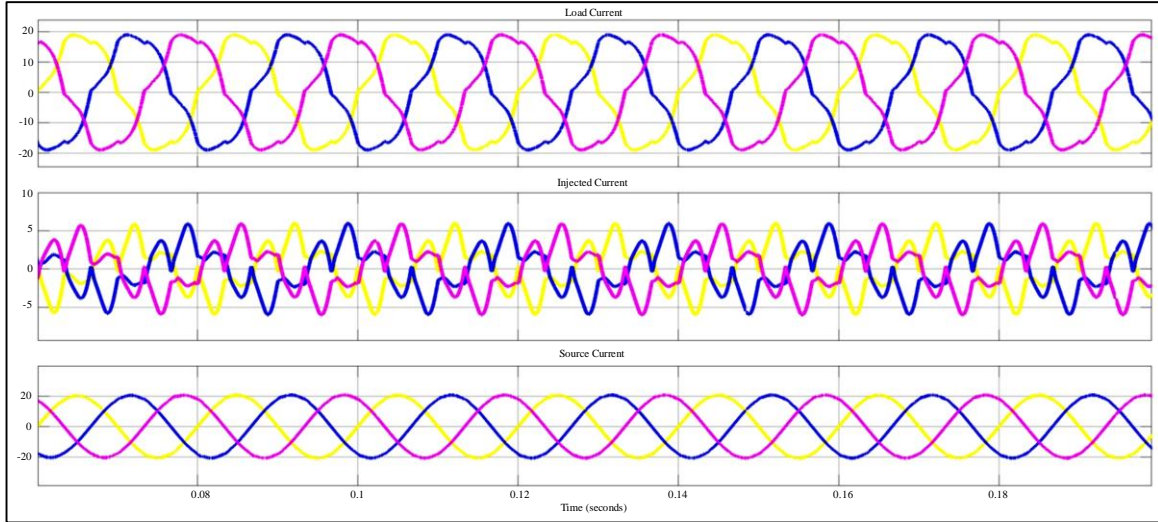
(a) Grid power, P_{PV} , P_{BESS} , P_w , P_{EV} , P_L



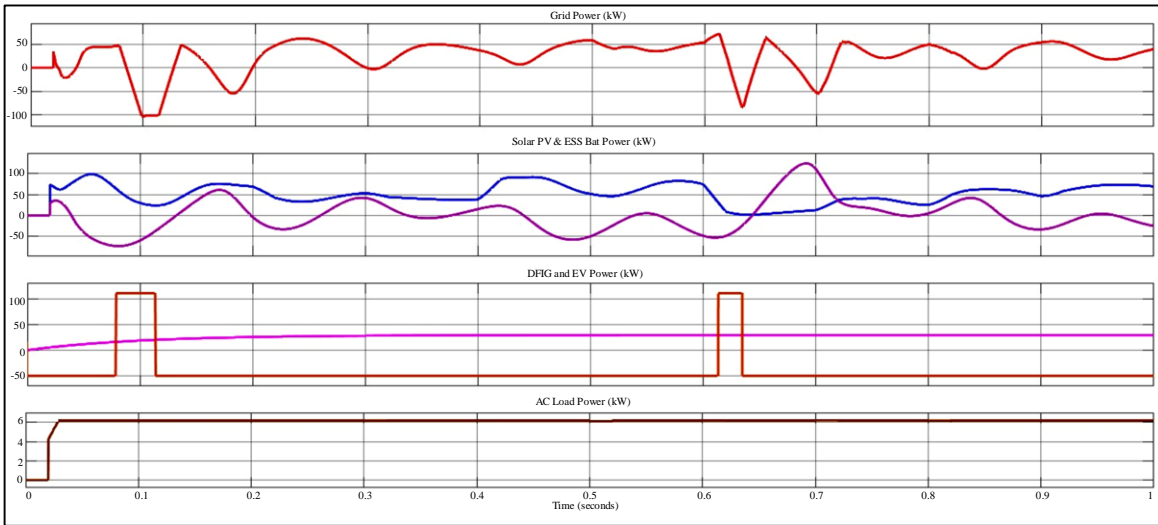
(b) G , P_{PV} , UPQC DC link voltage



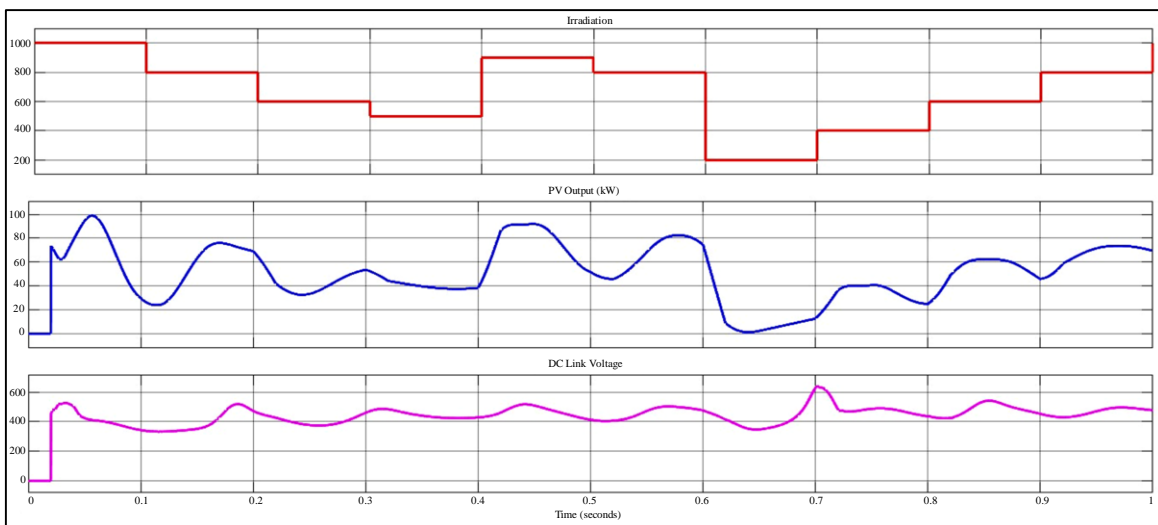
(c) Grid voltage, load voltage, series filter compensated voltage



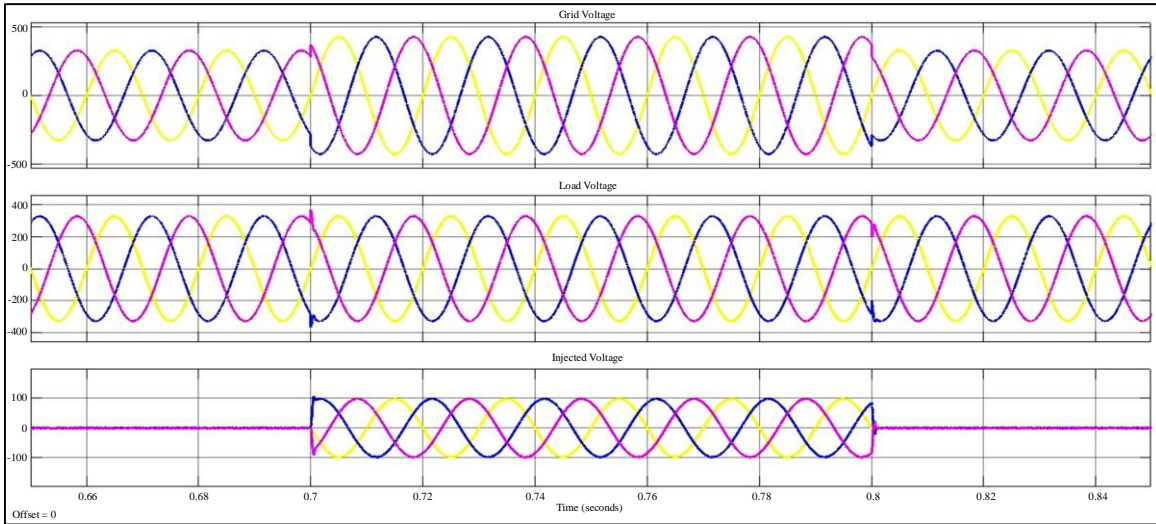
(d) Current at load, compensated current, source current
 Fig. 21 Waveforms of the developed method for case 2



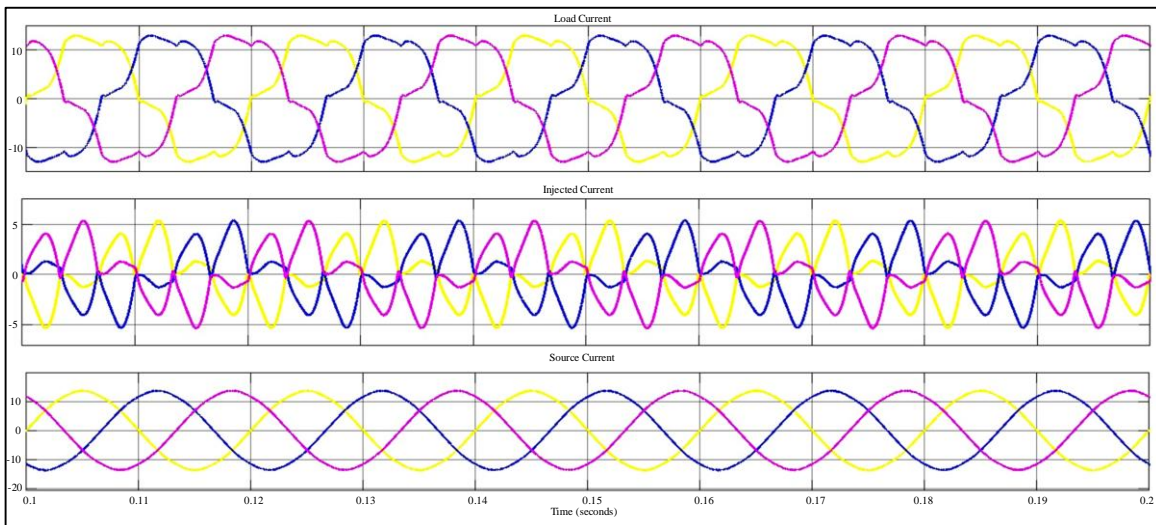
(a) Grid power, P_{PV} , P_{BESS} , P_w , P_{EV} , P_L



(b) G , P_{PV} , UPQC DC link voltage



(C) Grid voltage, load voltage, series filter compensated voltage



(d) Current at load, compensated current, source current
Fig. 22 Waveforms of the developed method for case 3

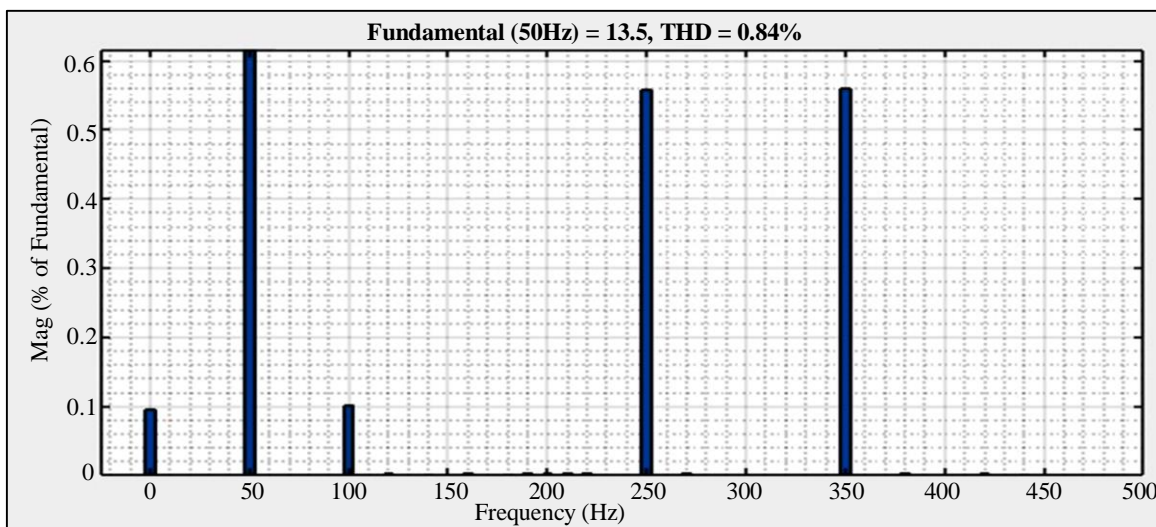


Fig. 23 Current %THD spectrum for phase-a case1

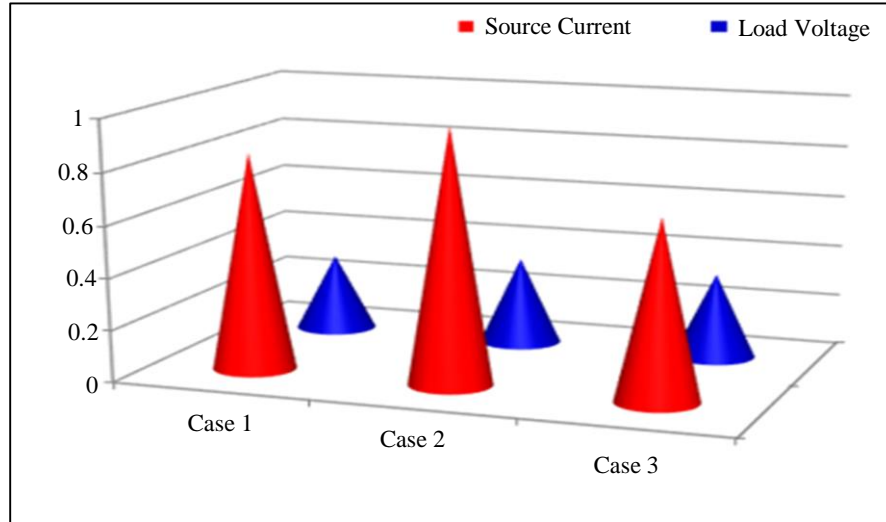


Fig. 24 %THD comparison

6. Conclusions

The developed approach was introduced to intelligently manage power in a system comprising SPV, WES, BESS, and EVs using an ANFIS-based EVA. The ANFIS hybrid method is also employed as the MPPT method in the SPV system to extract the highest available power. Furthermore, beyond power management, the system effectively addresses PQ concerns through UPQC controllers. Here, UPQC offers DC link regulation for variable load and irradiation conditions. An EVA is suggested to supply load demand and accommodate the necessary number of EVs to enhance the integration of

weather-dependent SPV systems. This proposed system ensures efficient power management and improves power quality by incorporating EVs into the grid. Notably, the system effectively mitigates voltage distortions such as sags, swells, disturbances, and current waveform imperfections, UPQC in conjunction with RES, BESS, and EVs. The levels of THD for voltages and currents have been measured and found to be below 0.84% using this developed method. This research's findings can serve as a foundation for future work, potentially involving adopting metaheuristic algorithms for further enhancements in the EVA system.

References

- [1] Rajvikram Madurai Elavarasan, "Comprehensive Review on India's Growth in Renewable Energy Technologies in Comparison with Other Prominent Renewable Energy Based Countries," *Journal of Solar Energy Engineering*, vol. 142, no. 3, pp. 1-11, 2020. [[CrossRef](#)] [[Google Scholar](#)] [[Publisher Link](#)]
- [2] Rajvikram Madurai Elavarasan et al., "SWOT Analysis: A Framework for Comprehensive Evaluation of Drivers and Barriers for Renewable Energy Development in Significant Countries," *Energy Reports*, vol. 6, pp. 1838-1864, 2020. [[CrossRef](#)] [[Google Scholar](#)] [[Publisher Link](#)]
- [3] Rajvikram Madurai Elavarasan et al., "A Holistic Review of the Present and Future Drivers of the Renewable Energy Mix in Maharashtra, State of India," *Sustainability*, vol. 12, no. 16, pp. 1-33, 2020. [[CrossRef](#)] [[Google Scholar](#)] [[Publisher Link](#)]
- [4] G.M. Shafiullah, Mohammad Taufiqul Arif, and Amanullah M.T. Oo, "Mitigation Strategies to Minimize Potential Technical Challenges of Renewable Energy Integration," *Sustainable Energy Technologies and Assessments*, vol. 25, pp. 24-42, 2018. [[CrossRef](#)] [[Google Scholar](#)] [[Publisher Link](#)]
- [5] L. Ashok Kumar, and V. Indragandhi, "Power Quality Improvement of Grid Connected Wind Energy System Using Facts Devices," *International Journal of Ambient Energy*, vol. 41, no. 6, pp. 631-640, 2020. [[CrossRef](#)] [[Google Scholar](#)] [[Publisher Link](#)]
- [6] Shazly A. Mohamed, "Enhancement of Power Quality for Load Compensation Using Three Different Facts Devices Based on Optimized Technique," *International Transactions on Electrical Energy Systems*, vol. 30, no. 3, 2020. [[CrossRef](#)] [[Google Scholar](#)] [[Publisher Link](#)]
- [7] Sayan Paramanik, "Smart Grid Power Quality Improvement Using Modified UPQC," *2019 Devices for Integrated Circuit (DevIC)*, Kalyani, India, pp. 356-360, 2019. [[CrossRef](#)] [[Google Scholar](#)] [[Publisher Link](#)]
- [8] Pedro Nunes, and M.C. Brito, "Displacing Natural Gas with Electric Vehicles for Grid Stabilization," *Energy*, vol. 141, pp. 87-96, 2017. [[CrossRef](#)] [[Google Scholar](#)] [[Publisher Link](#)]
- [9] Peng-Yong Kong, and George K. Karagiannidis, "Charging Schemes for Plug-in Hybrid Electric Vehicles in Smart Grid: A Survey," *IEEE Access*, vol. 4, pp. 6846-6875, 2016. [[CrossRef](#)] [[Google Scholar](#)] [[Publisher Link](#)]
- [10] C. Chellaswamy, and R. Ramesh, "Future Renewable Energy Option for Recharging Full Electric Vehicles," *Renewable and Sustainable Energy Reviews*, vol. 76, pp. 824-838, 2017. [[CrossRef](#)] [[Google Scholar](#)] [[Publisher Link](#)]

- [11] Amirullah et al., "Load Active Power Transfer Enhancement Using UPQC-PV-BES System with Fuzzy Logic Controller," *International Journal of Intelligent Engineering and Systems*, vol. 13, no. 2, pp. 329-349, 2020. [[Google Scholar](#)] [[Publisher Link](#)]
- [12] Francisco José Vivas et al., "Multi-Objective Fuzzy Logic-Based Energy Management System for Microgrids with Battery and Hydrogen Energy Storage System," *Electronics*, vol. 9, no. 7, pp. 1-23, 2020. [[CrossRef](#)] [[Google Scholar](#)] [[Publisher Link](#)]
- [13] Koganti Srilakshmi et al., "Design of Soccer League Optimization Based Hybrid Controller for Solar-Battery Integrated UPQC," *IEEE Access*, vol. 10, pp. 107116-107136, 2022. [[CrossRef](#)] [[Google Scholar](#)] [[Publisher Link](#)]
- [14] Koganti Srilakshmi et al., "Design of UPQC with Solar PV and Battery Storage Systems for Power Quality Improvement," *Cybernetics and Systems, an International Journal*, 2023. [[CrossRef](#)] [[Google Scholar](#)] [[Publisher Link](#)]
- [15] Koganti Srilakshmi, Arun Nambi Pandian, and Aravindhababu Palanivelu, "Fuzzy Based Hybrid Controller for UPQC with Wind and Battery Storage Systems," *International Journal of Electronics*, pp. 1-26, 2023. [[CrossRef](#)] [[Google Scholar](#)] [[Publisher Link](#)]
- [16] Alapati Ramadeviet al., "Optimal Design and Performance Investigation of Artificial Neural Network Controller for Solar- and Battery-Connected Unified Power Quality Conditioner," *International Journal of Energy Research*, vol. 2023, pp. 1-22, 2023. [[CrossRef](#)] [[Google Scholar](#)] [[Publisher Link](#)]
- [17] Koganti Srilakshmi et al., "Optimal Design of an Artificial Intelligence Controller for Solar-Battery Integrated UPQC in Three Phase Distribution Networks," *Sustainability*, vol. 14, no. 21, pp. 1-30, 2022. [[CrossRef](#)] [[Google Scholar](#)] [[Publisher Link](#)]
- [18] Srilakshmi Koganti, Krishna Jyothi Koganti, and Surender Reddy Salkuti, "Design of Multi-Objective-Based Artificial Intelligence Controller for Wind/Battery-Connected Shunt Active Power Filter," *Algorithms*, vol. 15, no. 8, pp. 1-23, 2022. [[CrossRef](#)] [[Google Scholar](#)] [[Publisher Link](#)]
- [19] Koganti Srilakshmi et al., "Artificial Intelligence Based Multi-Objective Hybrid Controller for PV-Battery Unified Power Quality Conditioner," *International Journal of Renewable Energy Research*, vol. 12, no. 1, pp. 495-504, 2022. [[Google Scholar](#)] [[Publisher Link](#)]
- [20] Koganti Srilakshmi et al., "Design and Performance Analysis of Fuzzy Based Hybrid Controller for Grid Connected Solar-Battery Unified Power Quality Conditioner," *International Journal of Renewable Energy Research*, vol. 13, no. 1, pp. 1-13, 2023. [[Google Scholar](#)] [[Publisher Link](#)]
- [21] Koganti Srilakshmi et al., "Performance Analysis of Artificial Intelligence Controller for PV and Battery Connected UPQC," *International Journal of Renewable Energy Research*, vol. 13, no. 1, pp. 155-170, 2023. [[CrossRef](#)] [[Google Scholar](#)] [[Publisher Link](#)]